ORIGINAL ARTICLE

WILEY

Characterization of genetic humanized mice with transgenic HLA DP401 or DRA but deficient in endogenous murine MHC class II genes upon *Staphylococcus aureus* pneumonia

Feng Li 🆔 | Bowen Niu | Lingling Liu | Mengmin Zhu | Hua Yang | Boyin Qin | Xiuhua Peng | Lixiang Chen | Chunhua Xu | Xiaohui Zhou

Department of Laboratory Animal Science, Shanghai Public Health Clinical Center, Shanghai, China

Correspondence
Feng Li and Xiaohui Zhou, Department of Laboratory Animal Science, Shanghai Public Health Clinical Center, Shanghai 201508, China.
Email: lifeng30286@shaphc.org and zhouxiaohui@fudan.edu.cn

Abstract

Background: *Staphylococcus aureus* can cause serious infections by secreting many superantigen exotoxins in "carrier" or "pathogenic" states. *HLA DQ* and *HLA DR* humanized mice have been used as a small animal model to study the role of two molecules during *S. aureus* infection. However, the contribution of *HLA DP* to *S. aureus* infection is unknown yet.

Methods: In this study, we have produced *HLA DP401* and *HLA DRA0101* humanized mice by microinjection of C57BL/6J zygotes. *Neo-floxed IA$\beta^{+/-}$* mice were crossbred with Ella-Cre and further crossbred with *HLA DP401* or HLA-DRA0101 humanized mice. After several rounds of traditional crossbreeding, we finally obtained HLA *DP401-IA$\beta^{/-}$* and *HLA DRA-IA$\beta^{/-}$* humanized mice, in which human *DP401* or *DRA0101* molecule was introduced into *IA$\beta^{/-}$* mice deficient in endogenous murine MHC class II molecules. A transnasal infection murine model of *S. aureus* pneumonia was induced in the humanized mice by administering 2×10^8 CFU of *S. aureus* Newman dropwise into the nasal cavity. The immune responses and histopathology changes were further assessed in lungs in these infected mice.

Results: We evaluated the local and systemic effects of *S. aureus* delivered intranasally in *HLA DP401-IA$\beta^{/-}$* and HLA DRA-IA$\beta^{-/-}$ transgenic mice. *S. aureus* Newman infection significantly increased the mRNA level of *IL 12p40* in lungs in humanized mice. An increase in IFN-γ and IL-6 protein was observed in *HLA DRA-IA$\beta^{/-}$* mice. We observed a declining trend in the percentage of F4/80$^+$ macrophages in lungs in *HLA DP401-IA$\beta^{/-}$* mice and a decreasing ratio of CD4$^+$ to CD8$^+$ T cells in lungs in IA$\beta^{-/-}$ mice and *HLA DP401-IA$\beta^{/-}$* mice. A decreasing ratio of Vβ3$^+$ to Vβ8$^+$ T cells was also found in the lymph node of *IA$\beta^{/-}$* mice and *HLA DP401-IA$\beta^{/-}$* mice. *S. aureus* Newman infection resulted in a weaker pathological injury in lungs in *IA$\beta^{/-}$* genetic background mice.

Conclusion: These humanized mice will be an invaluable mouse model to resolve the pathological mechanism of *S. aureus* pneumonia and study what role DP molecule plays in *S. aureus* infection.

KEYWORDS

HLA DP401, HLA-DRA, humanized mice, MHC II, *Staphylococcus aureus* pneumonia, transgene

1 | INTRODUCTION

Staphylococcus aureus is an important bacterial pathogen in humans[1,2] and can cause severe tissue infection, including endocarditis, osteomyelitis, pneumonia, and sepsis.[1] Due to less protective immune responses, recurrent infections, and appearance of multidrug-resistant strains, *S aureus* has become the main reason for both hospital- and community-associated infections.[3]

As yet, one of the major challenges in studying the infectious mechanism of *S. aureus* is the lack of suitable animal models. Mouse is still the preferred animal model for the study of infectious diseases.[4–7] For the past 40 years, humanized mice have been used as a model to identify the function of SAgs during *S. aureus* infection. Compared to murine MHC class II molecules, human HLA molecules generally have stronger affinity to SAgs.[8] Intranasal exposure to *S. aureus* SAgs, such as staphylococcal enterotoxin B (SEB) and streptococcal pyrogenic exotoxin A (SPEA), can cause airway inflammation and systemic immune activation in *HLA DR2* and *DQ8* transgenic mice.[9] In a bacteremia model of *S. aureus* Newman with *HLA DR4* transgenic mice, researchers found that *S. aureus* can improve its survival in the liver by subverting the neutrophil response and accelerating abscess formation in a staphylococcal enterotoxin A (SEA)-dependent manner.[10] With *HLA DR4* transgenic mice, Szabo et al. found that invariant natural killer T cells play a pathogenic role in toxic shock syndrome and may be regarded as a potential therapeutic target in superantigen-mediated diseases.[11] However, those transgenic *HLA DQ* and *HLA DR* humanized mice were produced from HLA genes alone without the human regulatory elements for those genes. Therefore, they cannot mimic the transcriptional regulatory process in humans and might result in the artificial expression level of transgenes in mice.

Unlike the situation with *HLA DR* and *HLA DQ*,[12] knowledge of *HLA DP* alleles' role in SAgs during *S. aureus* infection is relatively limited. It is generally agreed that there is less importance for HLA-DP molecules in the immune response than for *HLA-DR* or *HLA-DQ* molecules, because previous studies have found that HLA-DP expression is ~10-fold lower than *HLA DQ* or *HLA DR* expression in the cell surface.[13–15] However, a majority of studies show that *HLA DP* genes can play a certain immunological role in cancer, allergy, and infectious disease, probably similar to DR or DQ gene.[16–20] In a previous study, we produced a *HLA DP401* transgenic mice carrying the whole DP gene locus.[21] Here, we also produced a *HLA DRA0101* transgenic mice containing the whole DRA genomic region. We further backcross those two mice in the genetic background of $IA\beta^{-/-}$ mice, which lack the endogenous murine MHC class II genes. With those humanized mice in the $IA\beta^{-/-}$ genetic background, that is, *HLA DP401-IA$\beta^{-/-}$* and *HLA DRA-IA$\beta^{-/-}$* mice, we developed a pneumonia mouse model by intranasal exposure to *S. aureus* Newman. The phenotypic characterization of these humanized mice in $IA\beta^{-/-}$ genetic background was further investigated.

2 | MATERIALS AND METHODS

2.1 | Production of HLA DRA transgenic mice

We obtained BAC CH501-213L12 with the *HLA DRA*0101* gene locus from the BACPAC resources. The preparation and purification of BAC DNA were as previously reported.[21] Pulsed field gel electrophoresis was used to check the integrity of BAC DNA after digestion with restriction endonucleases SacII or XhoI. Then, 1–3 ng/μL of circular BAC DNA diluted in microinjection buffer was microinjected into the pronuclei of C57BL/6 mouse zygotes. Positive F0 generations and hybridization progenies were genotyped in the following specific primers.

HLA DRA ex3-5, 5′-GGGGTATGGACCAACACTCA-3′ (forward) and 5′-AAGGCAATAGACAGGGAAGC-3′ (reverse) 1505 bp; 213L12-up-1, 5′-AACAACTACTGTGGGACTGC-3′ (forward) and 5′-AAGCC AAAGACAAGAAAGAT-3′ (reverse) 850 bp; 213L12-up-2, 5′-TACTG GGTTGAAAGGGAGAC-3′ (forward) and 5′-AGATAGAGGGAGGC TGGTGT-3′ (reverse) 962 bp; 213L12-down-1, 5′-AGGCAATGGGA TAAGACAAA-3′ (forward) and 5′-GGAAACCTGATGGAGGAAGA-3′ (reverse) 930 bp; 213L12-down-2, 5′-GTTAGACTGAACATAGG AGGAT-3′ (forward) and 5′-ACATAGCACTGTATTGGGAC-3′ (reverse) 750 bp.

2.2 | Mouse strains

HLA DP401 or *HLA DRA* humanized mice without MCH class II molecules (IAβ$^{-/-}$) were produced using backcross strategy, as previously reported.[21] EIIa-Cre mice,[22] IAβ[23] neo floxed mutant mice, and *HLA DP401-IA$\beta^{-/-}$* and *HLA DRA-IA$\beta^{-/-}$* mice were bred within the animal facility of Shanghai Public Health Clinical Center (SHPHC). C57BL/6J (wild-type [WT]) mice were purchased from Shanghai SLAC Laboratory Animal Co., Ltd. All experiments were approved by the Animal Ethics Committee of SHPHC (2020-A024-01).

2.3 | RNA isolation, cDNA synthesis, and reverse transcription-polymerase chain reaction (RT-PCR)

RNA was isolated from the peripheral blood mononuclear cell (PBMC), spleen, kidney, gut, and lung using TRleasy Total RNA Extraction Reagent (Yeasen, Shanghai). Reverse transcription RNA and cDNA synthesis was performed using a Hifair II First Strand cDNA synthesis kit (gDNA digester plus) (Yeasen), RT-PCR was amplified with TransTaq DNA Polymerase High Fidelity (Yeasen), and all the steps were followed according to the manufacturer's protocol. Primer sequences used and the predicted amplification sizes are as follows: HLA-DRA, 5′-TCCGCAAGTTCCACTATCTCC-3′ (forward) and 5′-CCATCACCTCCATGTGCCTTA-3′ (reverse) 275 bp.

2.4 | Bacterial strains, growth conditions, and *S. aureus* pneumonia model

S. aureus stain Newman was obtained from Prof. Minggui Wang at Huashan Hospital affiliated to Fudan University, Shanghai, China. Bacteria were grown aerobically at 37°C in tryptic soy broth (Difco) with shaking (250 rpm). Bacterial growth curves were measured using a microspectrophotometer system (K5600). Then the bacteria at exponential growth phase were harvested by centrifugation, washed and resuspended in phosphate-buffered saline (PBS), and then adjusted to a final concentration.

The infection murine model of *S. aureus* was produced as previously described by Bubeck Wardenburg.[24] Briefly, 8-week-old C57BL/6, *HLA DP401-IAβ$^{-/-}$* mice, *HLA DRA-IAβ$^{-/-}$* mice, and *IAβ$^{-/-}$* mice were intranasally infected with 2×10^8 CFU of *S. aureus* (50 μL). After 1, 3, and 7 days postinfection, mice were killed, and PBMC, lymph nodes, and lungs were aseptically harvested for further analysis.

2.5 | Expression analysis of transgenic mice using real-time PCR

Quantitative real-time PCR (QPCR) was performed to detect the mRNA level of cytokines and SEA, as described previously.[21] qPCR SYBR Green Master Mix (Yeasen) was used in these experiments. The primer sequences and product sizes are as follows: IFN-γ, 5′-AGCAACAGCAAGGCGAAAA-3′ (forward) and 5′-CTGGACCT GTGGGTTGTTGA-3′ (reverse) 71 bp; TNFα, 5′-CTTCTCATTCC TGCTTGTGG-3′ (forward) and 5′-ATCTGAGTGTGAGGGTCTGG-3′ (reverse) 140 bp; IL-6, 5′-CCGCTATGAAGTTCCTCTC-3′ (forward) and 5′-GGTATCCTCTGTGAAGTCTC-3′ (reverse) 122 bp; MCP-1, 5′-CTCTTCCTCCACCACCAT-3′ (forward) and 5′-CTCTCCAG CCTACTCATTG-3′ (reverse) 165 bp; IP-10, 5′-TTGAGATCATTGCC ACGAT-3′ (forward) and 5′-CTCTGCTGTCCATCCATC-3′ (reverse) 171 bp; IL-12p40, 5′-CAGAAAGGTGCGTTCCTCGTA-3′ (forward) and 5′-AAGCCAACCAAGCAGAAGACAG-3′ (reverse) 245 bp; MIP-2, 5′-GCAAGGCTAACTGACCTGGAA-3′ (forward) and 5′-CAACA

TCTGGGCAATGGAAT-3′ (reverse) 184 bp; 16s, 5′-GTAGGTGGCAA GCGTTAT-3′ (forward) and 5′-CATCAGCGTCAGTTACAGA-3′ (reverse) 228 bp; RANIII, 5′-TGATGGAAAATAGTTGATGAGTTGT-3′ (forward) and 5′-GTAGGTGGCAAGCGTTAT-3′ (reverse) 349 bp; sea, 5′-TTGGAAACGGTTAAAACGAA-3′ (forward) and 5′-GAACCTTC CCATCAAAAACA-3′ (reverse) 101 bp. The mRNA fold change of the purpose gene was computed using the conventional $2^{-\Delta\Delta Ct}$ method relative to the values in mock-treated samples after normalized to the expression value of housekeeping gene GAPDH.[25]

2.6 | Western blotting

Western blotting was performed as described previously.[26] Briefly, spleen homogenates were resuspended in cell lysis buffer (9803S, Cell Signaling). Protein lysates were purified before gel electrophoresis and further analyzed by 10% sodium dodecyl sulfate-polyacrylamide gel electrophoresis. Proteins were electrotransferred to polyvinylidene fluoride membranes, which were incubated with a monoclonal anti-DRA Ab and anti-β-actin Ab. Antibody-incubated membranes were further analyzed with a horseradish peroxidase–conjugated anti-rabbit IgG secondary Ab (ZSGB-BIO, Beijing, China) and ECL development (Pierce) according to the manufacturer's instructions.

2.7 | Enzyme-linked immunosorbent assay analysis of cytokine

Mice were killed at the indicated times, and pulmonary homogenates were lysed in RIPA lysis buffer (Beyontime, China). Lysates were stored at −80°C. Cytokine levels were detected using a mouse enzyme-linked immunosorbent assay (ELISA) kit (Solarbio, Beijing) and read on a Luminex 100 (Bio-Rad), as described in the manufacturer's instructions.

2.8 | Antibodies and flow cytometry analysis

The mice were euthanized by CO_2 3 days after infection. The lungs and inguinal lymph gland were isolated and then washed in PBS thrice. The lungs were cut into 1-mm^3 fragments, digested with collagenase IV for 45 min at 37°C, and terminated with an equal volume of RPMI-1640 complete medium. The digested lung fragments were filtered with a cell strainer and centrifuged at 500 g; then the supernatant was discarded, and the single cells were washed with PBS twice and finally resuspended with RPMI-1640 complete medium on ice. To acquire inguinal lymph node single cells, the nodes were ground slightly using the tail of the syringe without digestion and processed using the protocol as mentioned earlier; 1×10^6 cells were incubated with FcR-specific blocking mAb (eBioscience) for 15 min at 4°C and then stained with antibodies for 30 min at 4°C. The following antibodies were used: APC/Cyanine7-anti-mouse-CD45,

Alexa Fluor-anti-mouse CD3, Pacific Blue-anti-mouse CD4, Brilliant Violet 605-anti-mouse CD8, PE-anti-mouse Vβ3, FITC-anti-mouse Vβ8, APC-anti-mouse F4/80, PE/Cyanine7-anti-mouse-CD11B, FITC-LY6G, and Zombie Aqua fixable viability kit for distinguishing live and dead cells; all the antibodies and kit were purchased from Biolegend. The stained cells were washed with PBS twice and re-suspended with 200 μL of staining buffer; then they were examined using flow cytometry (LSRFortessa, BD Bioscience) and analyzed using FlowJo software.

2.9 | Histopathology and immunostaining procedure

For histological analysis, lung tissues were fixed, dehydrated, and finally embedded in paraffin and then cut into 5-μm-thick sections, as previously described.[21] Hematoxylin and eosin (H&E) staining was used for subsequent histopathological examination. Entire lung sections stained with H&E were automatically digitized and analyzed using the TissueFAXS200 tissue slide analysis system (TissueGnostics, Austria). These images were further evaluated based on a histopathologic inflammatory scoring system as described previously,[27] which has been widely employed to analyze many mouse models of respiratory infections.[28,29]

Routine protocol for immunohistochemical analysis was used in this study, as previously described.[21] Frozen lung tissues were immediately placed in 10% neutral formaldehyde fixative for 12 h and cryoprotected in 30% sucrose in PBS at 4°C overnight; 10- to 12-μm frozen sections were prepared using a cryostat. The polyclonal primary antibody used was specific for CD68 (GB113109, Servicebio, Wuhan, China) and Ly6g (GB11229, Servicebio). Staining against CD68 and Ly6g was performed using the standard immunohisto-chemical procedure with an avidin-biotin-peroxidase complex and 3,38-diaminobenzidine according to the manufacturer's instructions (Boster Biological Technology, Wuhan, China). After the primary antibody and the biotin-conjugated secondary antibody were added and incubated 45 min with strepavidin-biotin-complex (SABC) and then 5–10 min with 0.5 mg/mL super sensitive polymer-HRP ISH detection system (DAB solution), browning reaction products were derived in sections. Standard hematoxylin staining was further performed, and bright field images of the sections were obtained digitally.

2.10 | Statistical analysis

SPSS 21.0 software was used to analyze significant differences. Homogeneity of variance test and normality test was performed for the experimental data. If multiple sets of variables were consistent with homogeneity of variance, analysis of variance was used to compare multigroup variables, and least—significant difference (LSD) test was used to compare intergroup variables. If homogeneity of variance was not assumed, Dunnett's T3 test was used to compare intergroup variables. Values were represented as the mean ± standard deviation. Values of $p < 0.05$ were considered significant.

3 | RESULTS

3.1 | Generation of *HLA DP401-IAβ*$^{-/-}$ and *HLA DRA-IAβ*$^{-/-}$ humanized mice

In a previous study, we have produced *HLA DP401* humanized mice.[21] Here, *HLA DRA0101* humanized mice were further produced by microinjection of C57BL/6J zygotes with BAC clone CH501-213L12, which contained an entire *DRA0101* gene locus (Figure 1A). We obtained eight founder mice by thermal asymmetric interlaced-PCR analysis with specific oligonucleotides, which carried the entire exogenous transgene (Figure 1B). After founder mice were crossbred with WT mice (C57BL/6J), we finally obtained six F2 strains with the entire DRA gene. Total RNA of kidney and spleen was prepared from six F2 strains, and the DRA gene transcripts were found using RT-PCR in these tissues (Figure 1C). Western blot was further employed to investigate the expression of HLA DRA protein in the spleen. An intensive band was observed in the spleen from 134-4#, and a weaker band was also found in several other strains (Figure 1D). Then, total RNA was prepared from the gut, lungs, kidneys, thymus, and spleen of 134-4# offsprings, and DRA gene transcripts were verified using RT-PCR with specific oligo in these tissues (Figure 1E). This line was used in subsequent crossbreeding. In short, we produced the *HLA DRA* transgenic mice, and the transcription of HLA DRA gene was observed in the detected tissues from transgenic mice.

Then, homozygous IAβ$^{neo/neo}$ mice[23] were crossbred with Ella-Cre mice.[22] Ella-Cre mice were used to induce Cre-recombinase-mediated deletion. Murine MHC-II β chain (IAβ) gene was inactivated by traditional crossbreeding, and cell-surface expression of murine MHC-II IAβ was deleted. IAβ$^{+/-}$ mice with Ella-Cre were further crossbred with *HLA DP401* or *HLA DRA0101* humanized mice. After several rounds of traditional crossbreeding, we finally obtained *HLA DP401-IAβ*$^{-/-}$ and *HLA DRA-IAβ*$^{-/-}$ humanized mice, in which *DP401* or *DRA0101* molecule was introduced into IAβ$^{-/-}$ mice.

3.2 | Response of intranasal exposure to *S. aureus* Newman in IAβ$^{-/-}$ genetic background mice

To study the functionality of the *HLA DP401* and *DRA* molecules in mediating immune responses to *S. aureus* Newman infection, we established a transnasal infection murine model of *S. aureus* pneumonia in these humanized mice. After appropriate anesthesia, 2×10^8 CFU of *S. aureus* Newman was slowly administered dropwise into the nasal cavity.[24] All infected mice became sick, with symptoms of faster breathing, hunchbacked posture, drowsiness, and decreased activity at 24 h. *S. aureus* Newman infection resulted in a different number of deaths in each experimental group, that is, 1 of 11 in WT (C57BL/6J) mice, no death in IAβ$^{+/-}$ mice, three of 11 in

(A)

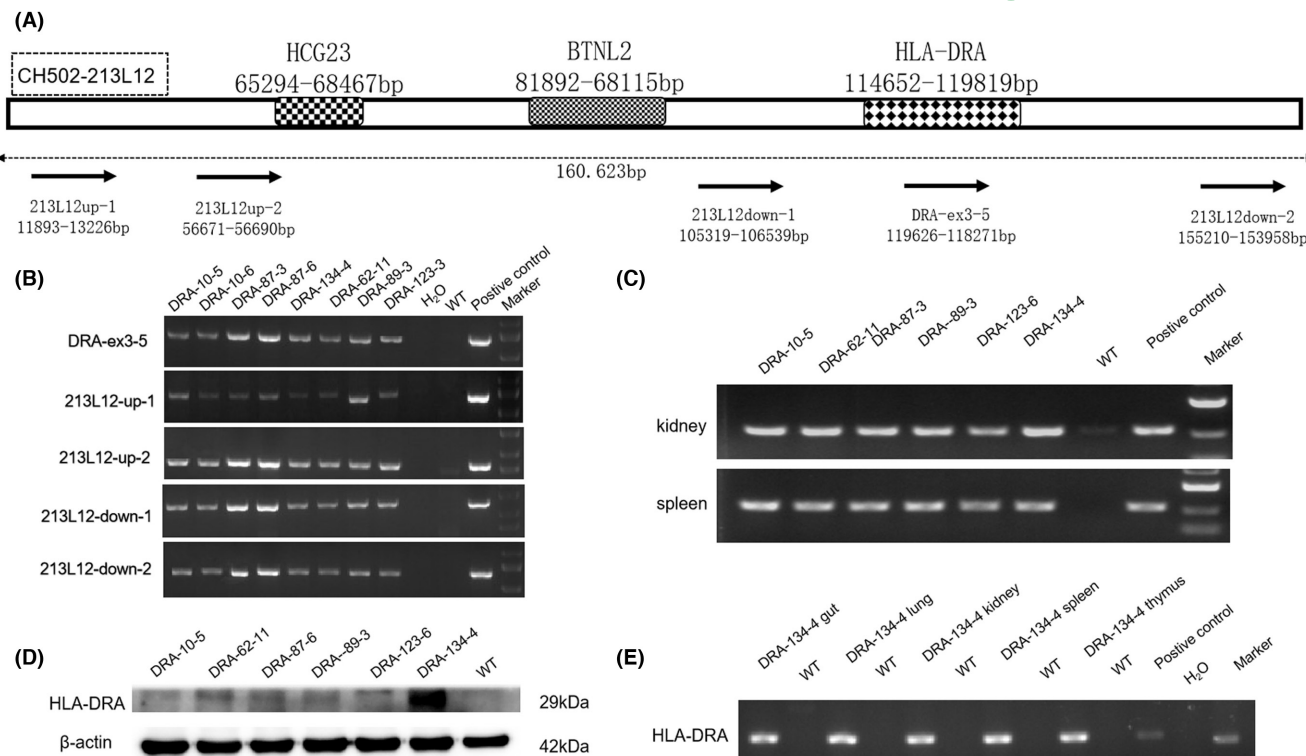**(B)**

(C)

(D)

(E)

FIGURE 1 Production of HLA DRA transgenic mice. (A) BAC CH502-213L12 containing HLA DRA gene locus and location of oligonucleotides used to genotype on BAC CH502-213L12. (B) Genotyping of several F2 transgenic mice with several pairs of primers designed specifically across the whole DRA gene locus. (C) The expression of HLA DRA was observed in spleen and kidney from six F2 strains using RT-PCR analysis. (D) Western blot analysis of the expression of HLA DRA in spleen from six F2 strains. (E) The transcripts of HLA DRA mRNA were observed in several tissues from one F2 strain using RT-PCR analysis.

HLA DP401-IA$\beta^{-/-}$ mice, and one of 11 in *HLA DRA-IA$\beta^{-/-}$* mice. The body weight of WT mice was significantly lower than that of IA$\beta^{-/-}$ mice at 24 h postinfection. The body weight of humanized mice appeared to be greater than that of WT mice (Figure S1A). The ratio of lung to weight did not significantly change among the four groups (Figure S1B). It is well known that *S. aureus* Newman can manufacture SEA in the process of the exponential phase of growth in vitro.[10] QPCR analysis showed that SEA expression was significantly higher in IA$\beta^{-/-}$ genetic background groups than in WT mice at 72 h postinfection (Figure S1C–E).

3.3 | *S. aureus* Newman infection induced production of IFN-γ and other cytokines in lungs

It is well known that SAgs are able to activate T cells by combining the T-cell receptor with MHC class II outside of the peptide binding grove and induce cytokine production.[30] Thus, we further detected cytokine expression to assess both local and systemic inflammation of infected mice 1 and 3 days postinfection (dpi). Lung homogenate and peripheral blood cells from Newman-infected mice were analyzed for several cytokines (Figure 2A–H). IFN-γ mRNA significantly increased 1 dpi in infected WT mice as well as 3 dpi in HLA DRA-IA$\beta^{-/-}$ mice (*p* < 0.05) mice (Figure 2A), whereas in *HLA DP401-IA$\beta^{-/-}$* mice, IFN-γ mRNA showed an increase at 3 dpi but without

a significant statistical difference (*p* = 0.066) (Figure 2A). Those observations confirmed previous reports that intranasal exposure to bacterial superantigen SEB induced an elevated level of IFN-γ in the BAL fluid of *HLA DR3* humanized mice.[9] TNFα mRNA significantly increased in WT mice and IA$\beta^{-/-}$ mice at 1 dpi (Figure 2B). We also observed the significant increase in IL-6 mRNA (Figure 2C), MCP-1 mRNA (Figure 2D), and MIP-2 mRNA (Figure 2E) in WT mice, whereas MCP-1 mRNA (Figure 2D) and MIP-2 mRNA (Figure 2E) in DRA-IA$\beta^{-/-}$ mice at 1 dpi showed an increasing trend but without statistic significances. Previous results have revealed the upregulation of the chemokines MIP-2 and MCP-1 in Newman-infected livers from a bacteremia model of *HLA DR4* humanized transgenic mice.[10] IL-4 expression significantly increased just in HLA-DP401-IA$\beta^{-/-}$ mice at 3 dpi, and the same as the expression of IL-10 at 1 dpi (Figure 2G,H). IL-12p40 expression was significantly upregulated in two humanized mice at the time point checked (Figure 2F). In addition, we checked the expression level of IFN-γ (Figure 2I), IL-12p40 (Figure 2J), and chemokine interferon-induced protein 10 (IP-10) (Figure 2K) in the sera of these infected mice and observed two- to threefold increase in IL-12p40 (Figure 2J) in IA$\beta^{-/-}$ mice.

To investigate whether IAβ knockout and introduction of human MHCII molecule affect the expression level of cytokine protein in lungs, we further detected the expression level of IFN-γ, IL-6, and TNFα proteins using ELISA in lungs at 3 dpi. Highest expression of IFN-γ protein was found in *HLA DRA-IA$\beta^{-/-}$* mice

(DRA-IAβ$^{-/-}$ 296.41±30.03 vs. WT 172.56±9.55, $p < 0.0001$; DP401-IAβ$^{-/-}$ 141.28±11.10, $p < 0.0001$, IAβ$^{-/-}$ 238.98±18.31, $p < 0.05$) (Figure 3A). Although the expression level of TNFα protein was high in HLA DRA-IAβ$^{-/-}$ mice, it was not statistically significant (DRA-IAβ$^{-/-}$ 190.17±17.97 vs. DP401-IAβ$^{-/-}$ 154.17±26.83, IAβ$^{-/-}$ 153.50±28.01) (Figure 3B). The highest expression of IL-6 protein
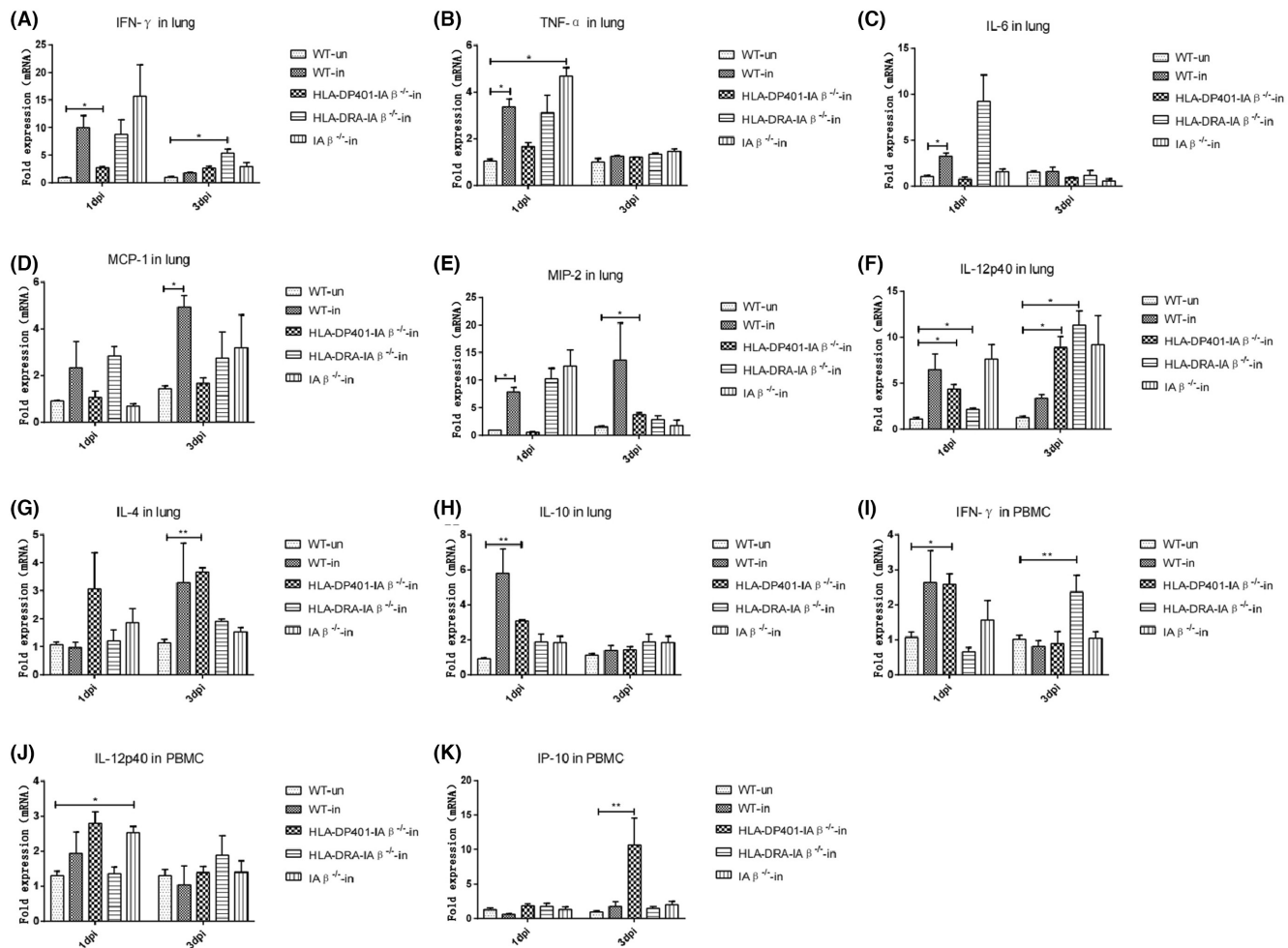

FIGURE 2 QPCR (quantitative PCR) checked the mRNA expression of cytokines induced by *Staphylococcus aureus* Newman infection. Peripheral blood cells and lung homogenates were collected from mice 24 and 72 h postinfection from *S. aureus* Newman–infected mice. Total RNA was extracted, and reverse transcription was performed using hot-resistance reverse transcriptase and random primers. Real-time PCR was used to analyze the expression level of cytokine mRNA with specifically designed oligonucleotides. Cytokines are labeled in the histogram. (A) INF-γ in lung, (B) TNFα in lung, (C) IL-6 in lung, (D) MCP-1 in lung, (E) MIP-2 in lung, (F) IL-12p40 in lung, (G) IL-4 in lung, (H) IL-10 in lung, (I) INF-γ in peripheral blood mononuclear cell (PBMC), (J) IL-12p40 in PBMC, and (K) IP-10 in PBMC. Data are shown as mean±SEM (standard error of the mean). Dunnett's *t*-test or LSD test was used to analyze significant differences ($p < 0.05$), which are denoted by asterisks.
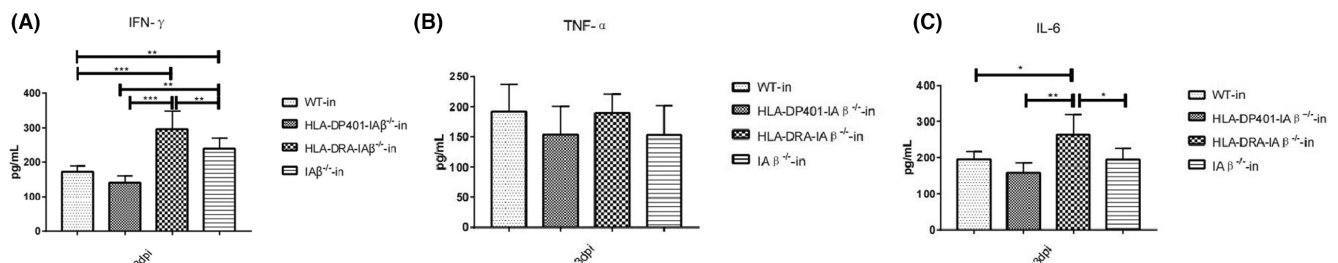

FIGURE 3 ELISA (enzyme-linked immunosorbent assay) analysis of the expression of cytokine protein induced by *S. aureus* Newman infection in lungs after *Staphylococcus aureus* Newman infection. The expression of (A) INF-γ, (B) TNFα, and (C) IL-6 protein in lung homogenate at 72 h postinfection. Data are shown as mean±SEM (standard error of the mean). LSD test was used to analyze significant differences ($p < 0.05$), which are denoted by asterisks.

was still observed in *HLA DRA-IAβ$^{-/-}$* mice (DRA-IAβ$^{-/-}$ 263.60±32.14 vs. WT 194.71±12.91, *p*<0.05; DP401-IAβ$^{-/-}$ 158.04±15.20, *p*<0.01; IAβ$^{-/-}$ 194.27±18.36, *p*<0.05) (Figure 3C).

3.4 | Immune characterization of *DP401-IAβ$^{-/-}$* and *HLA DRA-IAβ$^{-/-}$* humanized mice before and after *S. aureus* Newman infection

In a previous study, we observed the lower ratio of CD4$^+$ to CD8$^+$ T cells in thymus from *HLA DP401-IAβ$^{-/-}$* mice.[21] We further examined the composition of immune cell in lungs and lymph nodes of IAβ$^{-/-}$ mice and *HLA DRA-IAβ$^{-/-}$* and *HLA DP401-IAβ$^{-/-}$* mice. The ratio of CD4$^+$ to CD8$^+$ T cells in the lungs significantly decreased in

IAβ$^{-/-}$ genetic background mice than in WT mice (Figure 4A); as previously reported the ratio of CD4$^+$ to CD8$^+$ T cells in thymus from *HLA DR2-MHCII$^{-/-}$* mice was lower than that in WT mice.[31] Moreover, we observed the lower ratio of CD4$^+$ to CD8$^+$ T cells in the lungs from *HLA DP401-IAβ$^{-/-}$* mice compared to that from *HLA DRA-IAβ$^{-/-}$* mice. In addition, the difference was not statistically significant for the percentage of CD11b$^+$Ly6G$^+$ neutrophils (Figure 4B) and F4/80$^+$ macrophages (Figure 4C) among IAβ$^{-/-}$ genetic background mice and WT mice.

To investigate the potential effect of DPα/DPβ, DRα/Eβ, or Eα/Eβ molecules on maintaining T-cell homeostasis in the peripheral immune system, we continued to analyze the percentage of Vβ3$^+$ and Vβ8$^+$ T cells using flow cytometry in lymph nodes from IAβ$^{-/-}$ genetic background mice and WT mice. The percentage of Vβ3$^+$CD3$^+$
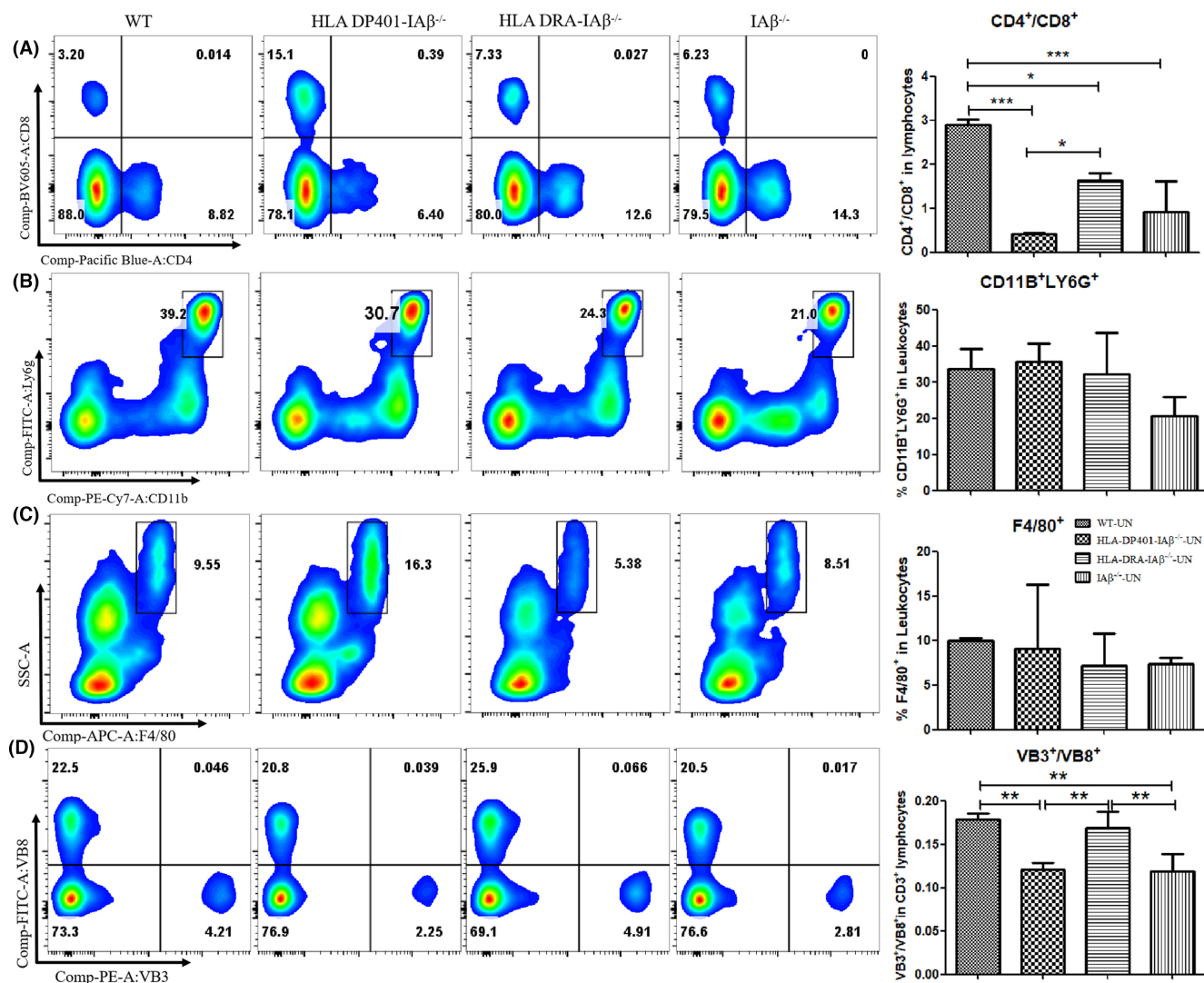

FIGURE 4 Flow cytometry of immune cells in naive humanized mice. (A) The ratio of CD4$^+$ to CD8$^+$ T cells in the lungs significantly decreased in IAβ$^{-/-}$ genetic background mice than in WT mice: The lower ratio of CD4$^+$ to CD8$^+$ T cells in the lungs from HLA DP401-IAβ$^{-/-}$ mice compared to that from HLA DRA-IAβ$^{-/-}$ mice. No statistically significant change in the percentage of (B) CD11B$^+$Ly6G$^+$ neutrophils and (C) F4/80$^+$ macrophages among IAβ$^{-/-}$ genetic background mice and WT mice. (D) The ratio of Vβ3$^+$ to Vβ8$^+$ T cells in the lymph nodes significantly decreased in IAβ$^{-/-}$ mice and HLA DP401-IAβ$^{-/-}$ mice than in WT mice: a significant increase in the ratio of Vβ3$^+$ to Vβ8$^+$ T cells in HLA DRA-IAβ$^{-/-}$ mice than in IAβ$^{-/-}$ mice and HLA DP401-IAβ$^{-/-}$ mice. Data are shown as mean±SEM (standard error of the mean). LSD test was used to analyze significant differences (*p*<0.05), which are denoted by asterisks.

T cells significantly decreased in IAβ$^{-/-}$ mice and *HLA DP401-IAβ$^{/-}$* mice compared to that in WT mice. We also observed the higher percentage of Vβ3$^+$CD3$^+$ T cells in *HLA DRA-IAβ$^{/-}$* mice compared to that in IAβ$^{-/-}$ mice and *HLA DP401-IAβ$^{/-}$* mice. Meanwhile, the higher percentage of Vβ8$^+$CD3$^+$ T cells was also detected in *HLA DRA-IAβ$^{/-}$* mice compared that in HLA DP401-IAβ$^{-/-}$ mice and WT mice. Thus, the ratio of Vβ3$^+$ to Vβ8$^+$ T cells significantly decreased in IAβ$^{-/-}$ mice and HLA DP401-IAβ$^{-/-}$ mice than in WT mice and *HLA DRA-IAβ$^{/-}$* mice (Figure 4D).

Because *S. aureus* Newman infection can rapidly induce the production of chemokines in the lungs of humanized mice, we speculated that the number of immunocytes recruited to the lungs would differ between humanized mice and WT mice. Macrophages and neutrophils are the body's first line of systemic defense against invasion by *S. aureus*,[32,33] and these populations were checked to evaluate whether *S. aureus* infection can result in a defect in phagocyte

recruitment. In addition, it is well known that lungs contain large numbers of resident macrophages,[34] so it was hypothesized that *S. aureus* Newman infection would affect the macrophage population. We isolated leukocytes from mouse lung at 3 dpi and employed various surface markers to perform flow analysis. We observed the lower ratio of CD4$^+$ to CD8$^+$ T cells in lungs from *HLA DP401-IAβ$^{/-}$* mice compared to that from WT mice (Figure 5A). The percentage of CD11b$^+$ Ly6G$^+$ neutrophils was not significantly altered among these mice infected with *S. aureus* Newman (Figure 5B). However, analysis of F4/80$^+$ macrophages revealed a declining trend in *HLA DP401-IAβ$^{/-}$* mice compared to IAβ$^{-/-}$ mice ($8.13\% \pm 1.60\%$ vs. $16.89\% \pm 4.51\%$, $p = 0.083$) (Figure 5C).

In addition, the percentage of Vβ3$^+$ and Vβ8$^+$ T cells was analyzed using flow cytometry in lymph nodes at 3 dpi. Newman-produced SEA is known to target Vβ3$^+$ T cells but not Vβ8$^+$ T cells.[35] Here, Vβ8$^+$CD3$^+$ T cells were regarded as an internal control.
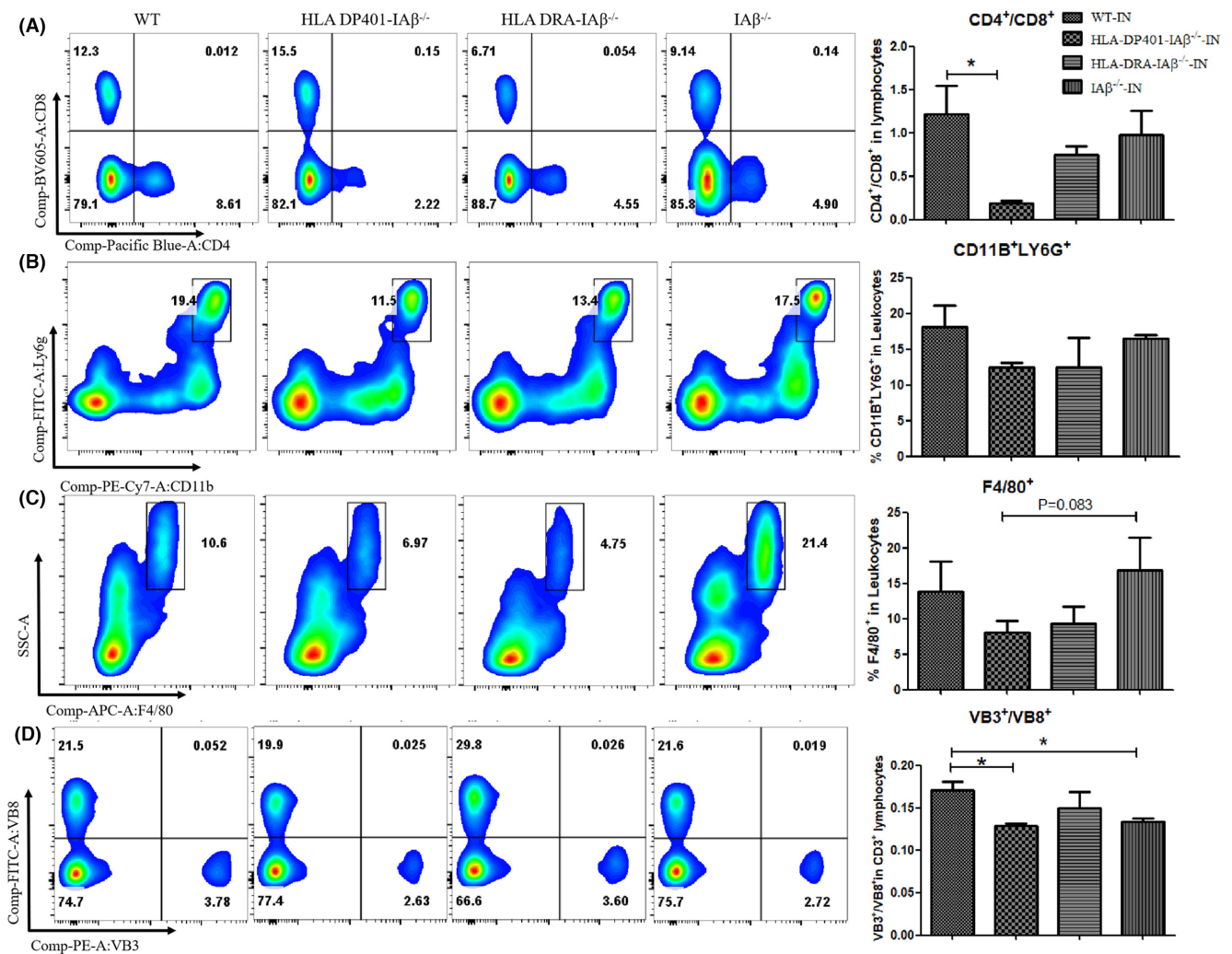

FIGURE 5 Flow cytometry of immune cells in humanized mice at 72 h after *Staphylococcus aureus* Newman infection. (A) The lower ratio of CD4$^+$ to CD8$^+$ T cells in the lungs from HLA DP401-IAβ$^{-/-}$ mice compared to that from WT mice. (B) No significant changes in the percentage of CD11b$^+$ Ly6G$^+$ neutrophils. (C) A declining trend in the percentage of F4/80$^+$ macrophages in HLA DP401-IAβ$^{-/-}$ mice compared to that in IAβ$^{-/-}$ mice. (D) The significant decrease in the ratio of Vβ3$^+$ to Vβ8$^+$ T cells in the lymph nodes of IAβ$^{-/-}$ mice and HLA DP401-IAβ$^{-/-}$ mice than in that of WT mice. Data are shown as mean $\pm$ SEM (standard error of the mean). LSD test was used to analyze significant differences ($p < 0.05$), which are denoted by asterisks.

The percentage of Vβ3⁺CD3⁺ T cells significantly decreased in *HLA DP401-IAβ$^{/-}$* mice compared to that in *HLA DRA-IAβ$^{/-}$* mice and WT mice. Moreover, the percentage of Vβ8⁺CD3⁺ T cells significantly increased in *HLA DRA-IAβ$^{/-}$* mice compared to that in *HLA DP401-IAβ$^{/-}$* mice, IAβ$^{-/-}$ mice, and WT mice (Figure 5D). Furthermore, we observed the significant decrease in the ratio of Vβ3⁺ to Vβ8⁺
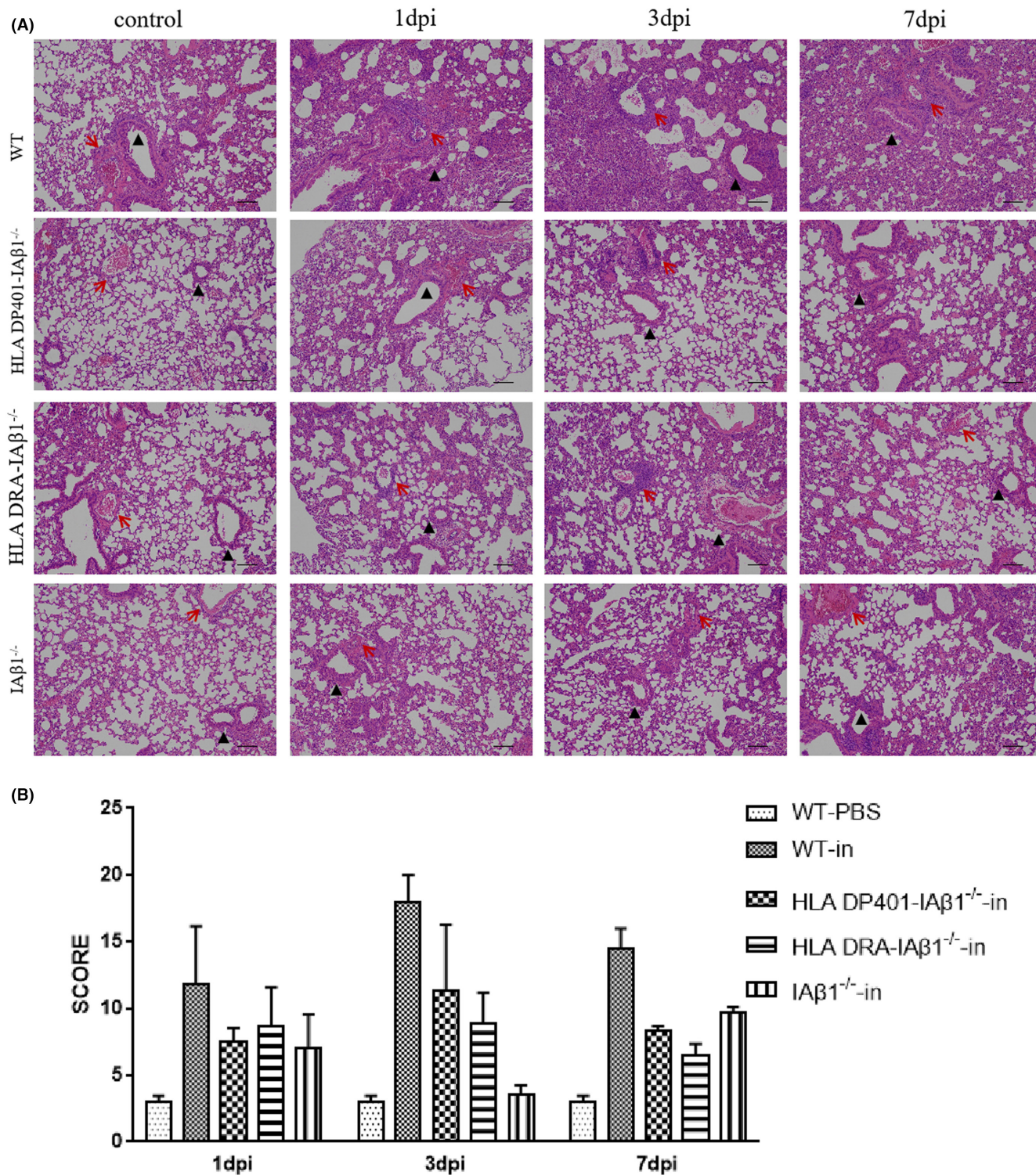

FIGURE 6 Histopathological changes in lungs after intranasal exposure to *Staphylococcus aureus* Newman. After intranasal exposure to *S. aureus* Newman, lung tissues were harvested at the time points labeled in the figure. Then, they were prepared and stained using hematoxylin and eosin solution. Representative histology for an uninfected control and an infected mice at the time point indicated is shown. The whole lung section was scanned, and six regions from each sample were selected and scored based on the distribution and character of pathologic alterations. Weak pathology was observed in IAβ$^{-/-}$ mice compared to WT mice. (A) Representative histopathological image; (B) histopathological score. Red arrow, blood vessel; black triangle, bronchioles. Scale bar: 100 μm. Data are shown as mean ± SEM (standard error of the mean). LSD test was used to analyze significant differences ($p < 0.05$).

T cells in IAβ$^{-/-}$ mice and *HLA DP401-IAβ$^{-/-}$* mice than in WT mice (Figure 5D).

3.5 | Pathological changes in lungs after *S. aureus* Newman infection

The lungs of infected humanized mice with *IAβ$^{-/-}$* genetic background were examined for gross pathology and histopathologic changes. The infected lungs were red, and the texture was firm (Figure S2). Histopathologic analysis was further employed to investigate the consequences of pulmonary infection with *S. aureus* in these mice. As previously reported,[24,36] transnasal infection with *S. aureus* Newman caused nonexpansive bronchopneumonia with multiple lesions and uneven lobular distribution. Severe damage was observed in the bronchi, alveoli, and interstitium. We also observed the large areas of necrosis and hemorrhage and the perivascular areas infiltrated by lymphocytes and neutrophils (Figure 6A; Figure S3A–D). Furthermore, H&E staining did not reveal the existence of staphylococci in the slide, which may be attributed to the low bacterial concentration in the lungs. The histology score is shown in Figure 6B and Table 1, revealing significant difference between *IAβ$^{-/-}$* genetic background mice and WT mice at 3 and 7 dpi postinfection, indicating that *S. aureus* Newman infection resulted in a weaker pathological injury in *IAβ$^{-/-}$* genetic background mice. Immunohistochemical analysis confirmed that *S. aureus* Newman infection caused a significant increase in Ly6G$^+$ neutrophils (Figure 7B,D) and CD68$^+$ macrophages (Figure 7A,C) in the time point checked compared to WT mice uninfected. In addition, immunohistochemical analysis showed that there was no significant change in Ly6G$^+$ neutrophils (Figure S4A,B) and CD68$^+$ macrophages (Figure S4A,C) in naive *IAβ$^{-/-}$* genetic background mice.

4 | DISCUSSION

It is well known that MHCII molecule plays pivotal roles in positive and negative selection of CD4$^+$ T cells in thymus. As previously reported, genetic deletion of murine MHCII A molecule caused a significant decrease in the ratio of CD4$^+$ to CD8$^+$ T cells in the thymus from IAβ$^{-/-}$ mice.[21] HLA DRA introduction into IAβ$^{-/-}$ genetic background mice can partially increase the ratio of CD4$^+$ to CD8$^+$ T cells in the thymus.[31] However, we still observed that the ratio of CD4$^+$ to CD8$^+$ T cells in the lungs from DRA-IAβ$^{-/-}$ mice could not be achieved for WT mice. As for *HLA DP401-IAβ$^{-/-}$* mice, the introduction of the HLA DP molecule into IAβ$^{-/-}$ genetic background mice did not improve the ratio of CD4$^+$ to CD8$^+$ T cells in the thymus[21] or in the lungs (Table 1). In addition, the ratio of Vβ3$^+$ to Vβ8$^+$ T cells did not improve in the lymph nodes from *HLA DP401-IAβ$^{-/-}$* mice. But the ratio of Vβ3$^+$ to Vβ8$^+$ T cells recovered to normal level in the lymph nodes from *HLA DRA-IAβ$^{-/-}$* mice. This indicates that only one functional murine MHCII E molecule present in the thymus would produce less-efficient CD4$^+$-positive selection, and less-efficient

TABLE 1 Summary of infection results in humanized mouse model.

	Index	Day 0	Day 1	Day 3	Day 7
WT	mRNA		TNFα↑, IL-6↑, MIP-2↑	TNFα↑ ($p=0.059$), MCP-1↑, IL-12p40↑ ($p=0.051$)	
	Histology score	3.0 ± 0.45	11.83 ± 4.34	18.0 ± 2.02	14.5 ± 1.5
HLA DP401-IAβ$^{-/-}$	mRNA		IFN-γ↑, IL-12p40↑, IL-10↑	IFN-γ↑ ($p=0.066$), TNFα↑ ($p=0.056$), IL-12p40↑, MIP-2↑, IL-4↑	
	Flow cytometry	CD4↓, CD4/CD8↓, Vβ3↓, Vβ3/Vβ8↓		CD4↓, CD4/CD8↓, Vβ3↓, Vβ3/Vβ8↓, F4/80↓ ($p=0.083$)	
	Histology score		7.5 ± 1.04	$11.33\pm4.95\downarrow$ ($p=0.089$)	$8.33\pm0.33\downarrow$
HLA DRA-IAβ$^{-/-}$	mRNA		MCP-1↑ ($p=0.080$), MIP-2↑ ($p=0.083$), IL-12p40↑	IFN-γ↑, TNFα↑ ($p=0.076$), IL-4↑ ($p=0.058$)	
	ELISA			IFN-γ↑, IL-6↑	
	Flow cytometry	CD4↓, CD4/CD8↓		CD4↑, CD8↑, Vβ3↑, Vβ8↑	
	Histology score		$8.67\pm5.06\downarrow$	$8.83\pm2.35\downarrow$	$6.5\pm1.5\downarrow$
IAβ$^{-/-}$	mRNA		TNFα↑	IL-6↑ ($p=0.085$), IL-10↑ ($p=0.075$) ELISA IFN-γ↑	
	Flow cytometry	CD4↓, CD4/CD8↓, Vβ8↓, Vβ3/Vβ8↓		Vβ3/Vβ8↓	
	Histology score		$7.0\pm2.57\downarrow$	$3.5\pm0.76\downarrow$	$9.67\pm0.76\downarrow$

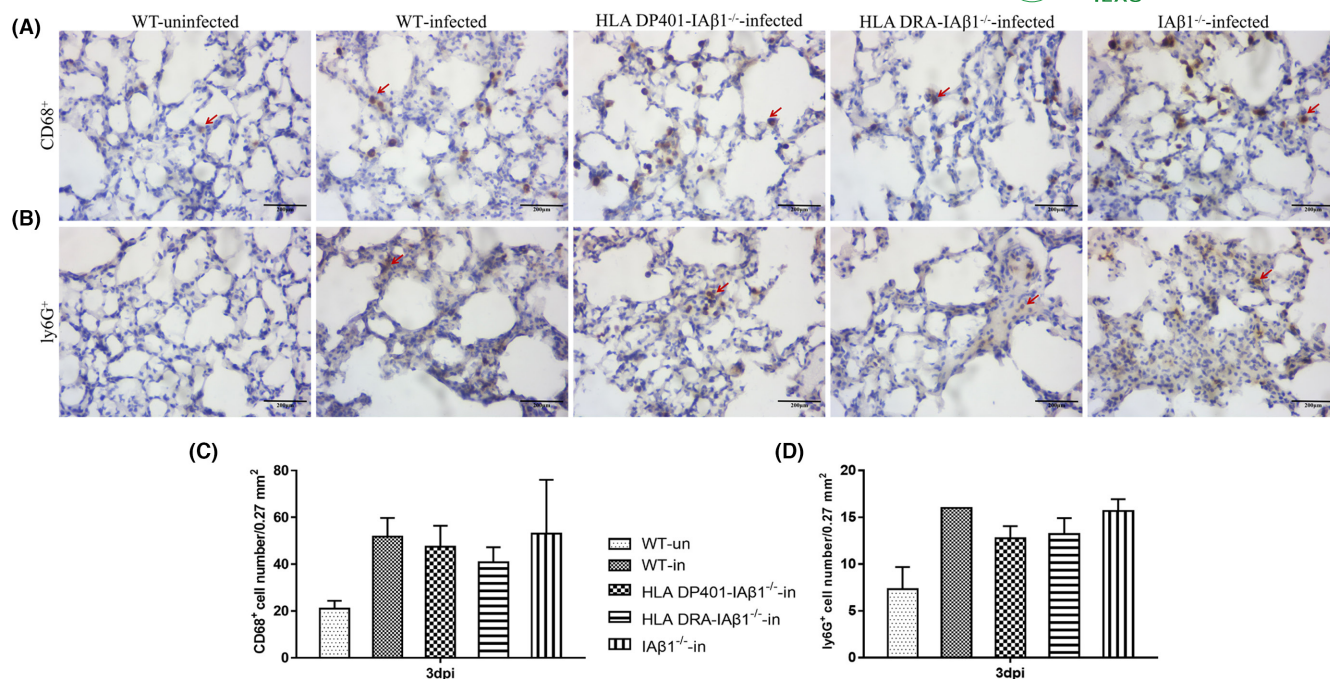Abbreviations: ELISA, enzyme-linked immunosorbent assay; WT, wild type.

FIGURE 7 *Staphylococcus aureus* Newman infection induced an increasing number of CD68⁺- and Ly6G⁺-positive cells in lungs. After intranasal exposure to *S. aureus* Newman, lung tissues were harvested at 72 h postinfection, and then 10-μm frozen sections were prepared. Immunohistochemistry was performed with (A) anti-CD68⁺ and (B) anti-Ly6G⁺, and the number of (C) CD68⁺- and (D) Ly6G⁺-positive cells in each slide was counted. Data are shown as mean ± SEM (standard error of the mean). Newman infection induced an increasing number of CD68⁺- and Ly6G⁺-positive cells in lungs. Red arrow, positive cells. Scale bar: 100 μm. Significant differences ($p < 0.05$) were determined by unpaired Student's *t*-test.

interaction would occur between murine CD4⁺ molecule and human MHCII DP molecule. *HLA DRA-IAβ⁻/⁻* humanized mice may express DRα/Eβ or Eα/Eβ, and HLA DP401-IAβ⁻/⁻ humanized mice may express DPα/DPβ and Eα/Eβ. DRα/Eβ molecule can be partially functional of murine MHCII A molecule, but DPα/DPβ molecule cannot. Humans have three classical class II molecules (HLA DP, HLA DQ, and HLA DR), and only two orthologous proteins (A and E molecules) are found in mice.[37] Given that there are different evolutionary patterns for three classical class II molecules,[38] the current results collectively indicate that HLA-DP molecule should have a different function from HLA DQ and HLA DR molecules.

Staphylococcal SAgs have been shown to be strongly related with pneumonia. In *S. aureus*–infected pneumonia, SAgs can participate in the formation of an unconventional T-cell activation complex by tightly coupling MHC class II to the TCR β-chain and stimulate a massive T-cell response independent of conventional antigen processing and presentation. In general, SAgs have a weak affinity for murine MHC II molecules compared to human HLA II molecules.[30] A previous study has shown that intranasal exposure to SEB can induce severe airway inflammation in HLA-DR3 transgenic mice than in BALB/c mice,[9] and airway inflammation and systemic immune activation are also observed in HLA-DQ8 transgenic mice after intranasal administration of SPEA.[9] An inverse SEB concentration effect was also observed for lymphocyte and macrophage recruitment in a HLA DR3-SEB inoculated model.[31] *S. aureus* Newman can enhance bacterial concentration in the liver

of *HLA DR4* transgenic mice by SEA-dependent Vβ skewing of T cells, and SEA can increase the infiltration of CD11b⁺Ly6G⁺ into the liver by elevating IFN-γ and IL-12 expression.[10] On the contrary, a previous study has also found that SAgs have a binding preference for different MHC II molecules[39]; for instance, DQ molecules are less efficient in presenting SEB compared to DR molecules,[31] and human DRA molecules have a strong affinity for SEA from Newman.[9] *S. aureus* CP8 activates CD4⁺ T cells to produce IFN-γ in an MHCII-dependent mechanism.[40] In this study, a decreasing trend was observed for the ratio of CD4⁺ to CD8⁺ in the lungs of HLA DRA mice before and after intranasal exposure to *S. aureus* Newman. No significant change was observed for the ratio of CD4⁺ to CD8⁺ in the lungs of HLA DP401 mice. For some unknown reason, we also observed a decreasing trend in the percentage of F4/80⁺ macrophage. In addition, a significant increase in IL-12p40 expression was observed in two humanized mice (Table 1). The current results may indicate that there are different roles for human DP and DRA molecules during *S. aureus* Newman infection. The whole DP gene locus, including the human DOA-DPA1-DPB1-DPB2 genomic region, was integrated into the mouse genome in *HLA DP-IAβ⁻/⁻* mice. There is no homologous region in mouse genome for human DP gene locus.[37] A previous study has revealed that two of five recombination hot spots in the human MHC II region are located at DP gene locus, namely DOA-DPA1 region and DPB1-DPB2 region.[41] We presumed that DP gene locus may also have unknown regulatory sequences, giving mice some

new human immunological characteristics. Of course, one murine E molecule was still expressed on the cell surface, and this may affect the experimental results in these humanized transgenic mice.

Here, the ratio of Vβ3[+] to Vβ8^{+} T cells in *HLA DRA-IAβ^{-/-}* mice was higher than that in *HLA DP401-IAβ^{-/-}* and *IAβ^{-/-}* mice before infection. But the ratio of Vβ3[+] to Vβ8^{+} T cells became similar among the IAβ^{-/-} genetic background mice after infection. Newman infection induced weak expansion of Vβ8^{+} T cells, which caused a slight decrease in the ratio of Vβ3[+] to Vβ8^{+} T cells in HLA DRA-IAβ^{-/-} mice. We compared the ratio of Vβ3[+] to Vβ8^{+} T cells before and after infection in these mice and did not find that SEA was specifically targeting the Vβ3^{+} T-cell population in this study, distinguishing from a previous study[10] that SEA interacted specifically with the Vβ3^{+}CD3^{+} T cells in the *S. aureus* bacteremia of HLA DR4-IE humanized mice. We speculate that differences in those factors, including mouse strain/substrain, animal model, bacterial strain, and doses and routes of inoculation, could affect the outcome of experimental results.

5 | CONCULSION

S. aureus is the main pathogen of human suppurative infection. Humanized mice have been used to establish the model of SAgs-induced airway inflammation,[9] which can efficiently investigate virulence contributions and vaccine efficacy of a specific antigen(s).[42] Both the size of the inoculum and the mouse strain used can contribute to the differences in pathological changes in pneumonia in the animal model.[4,24,43] Both α-toxin and protein A have also been described to have the ability to induce pulmonary inflammation, contributing to disease development.[24,44–46] Undoubtedly, many factors contribute to complicated pathological changes in this study. Previous studies have shown that the pathogenesis of *S. aureus* pneumonia is enhanced by CD4^{+} T cells, which affect the outcome of *S. aureus* infection by participating in IFN-γ-controlled chemokine production.[40,47] A defect in T-cell signaling in IAβ^{-/-} genetic background mice may attribute to a weaker pathological change. In summary, the humanized mouse model described here should provide a valuable tool to assess the role of staphylococcal virulence factors in the pathogenesis of pulmonary infection and study the role of DP molecules in *S. aureus* infection.

AUTHOR CONTRIBUTIONS

Feng Li and Xiaohui Zhou conceived and designed the study; Bowen Niu completed the microinjection and flow cytometry analysis; Lingling Liu was involved in immunostaining, histopathology, and Western blotting; Mengmin Zhu undertook the preparation of BAC clone and performed quantitative PCR and enzyme-linked immunosorbent assay for cytokine analysis; Hua Yang and Boyin Qin were involved in the mouse model of *S. aureus* pneumonia and sample collection; Xiuhua Peng, Lixiang Chen, and Chunhua Xu participated in transgenic animal breeding; Bowen Niu, Lingling Liu, and Mengmin Zhu plotted the figures; Feng Li and Xiaohui Zhou drafted the manuscript; all authors revised the final version.

CONFLICT OF INTEREST STATEMENT

The authors declare that they have no conflicts of interest to this work. Xiaohui Zhou is an editorial board member of *AMEM* and co-author of this article. To minimize bias, he was excluded from all editorial decision making related to the acceptance of this article for publication.

ETHICS STATEMENT

The study was approved by the Institute of Animal Use and Care Committee of Shanghai Public Health Clinical Center (GW2020-A024-01).

ORCID

Feng Li https://orcid.org/0000-0003-1291-5315

REFERENCES

1. Lowy FD. *Staphylococcus aureus* infections. *N Engl J Med*. 1998;339:520-532.
2. von Eiff C, Becker K, Machka K, Stammer H, Peters G. Nasal carriage as a source of *Staphylococcus aureus* bacteremia. Study group. *N Engl J Med*. 2001;344:11-16.
3. Chambers HF. Community-associated MRSA—resistance and virulence converge. *N Engl J Med*. 2005;352:1485-1487.
4. Kim HK, Missiakas D, Schneewind O. Mouse models for infectious diseases caused by *Staphylococcus aureus*. *J Immunol Methods*. 2014;410:88-99.
5. Lin L, Ibrahim AS, Xu X, et al. Th1-Th17 cells mediate protective adaptive immunity against *Staphylococcus aureus* and Candida albicans infection in mice. *PLoS Pathog*. 2009;5:e1000703.
6. Szabo EK, MacCallum DM. The contribution of mouse models to our understanding of systemic candidiasis. *FEMS Microbiol Lett*. 2011;320:1-8.
7. Wiles S, Hanage WP, Frankel G, Robertson B. Modelling infectious disease—time to think outside the box? Nature reviews. *Microbiology*. 2006;4:307-312.
8. Salgado-Pabon W, Schlievert PM. Models matter: the search for an effective *Staphylococcus aureus* vaccine. *Nat Rev Microbiol*. 2014;12:585-591.
9. Rajagopalan G, Iijima K, Singh M, Kita H, Patel R, David CS. Intranasal exposure to bacterial superantigens induces airway inflammation in HLA class II transgenic mice. *Infect Immun*. 2006;74:1284-1296.
10. Xu SX, Gilmore KJ, Szabo PA, et al. Superantigens subvert the neutrophil response to promote abscess formation and enhance *Staphylococcus aureus* survival in vivo. *Infect Immun*. 2014;82:3588-3598.
11. Szabo PA, Rudak PT, Choi J, et al. Invariant natural killer T cells are pathogenic in the HLA-DR4-transgenic humanized mouse model of toxic shock syndrome and can be targeted to reduce morbidity. *J Infect Dis*. 2017;215:824-829.
12. Taneja V, David CS. HLA class II transgenic mice as models of human diseases. *Immunol Rev*. 1999;169:67-79.

13. Edwards JA, Durant BM, Jones DB, Evans PR, Smith JL. Differential expression of HLA class II antigens in fetal human spleen: relationship of HLA-DP, DQ, and DR to immunoglobulin expression. *J Immunol*. 1986;137:490-497.

14. Guardiola J, Maffei A. Control of MHC class II gene expression in autoimmune, infectious, and neoplastic diseases. *Crit Rev Immunol*. 1993;13:247-268.

15. Hauber I, Gulle H, Wolf HM, Maris M, Eggenbauer H, Eibl MM. Molecular characterization of major histocompatibility complex class II gene expression and demonstration of antigen-specific T cell response indicate a new phenotype in class II-deficient patients. *J Exp Med*. 1995;181:1411-1423.

16. Caccamo N, Barera A, Di Sano C, et al. Cytokine profile, HLA restriction and TCR sequence analysis of human CD4+ T clones specific for an immunodominant epitope of *Mycobacterium tuberculosis* 16-kDa protein. *Clin Exp Immunol*. 2003;133:260-266.

17. de Waal L, Yuksel S, Brandenburg AH, et al. Identification of a common HLA-DP4-restricted T-cell epitope in the conserved region of the respiratory syncytial virus G protein. *J Virol*. 2004;78:1775-1781.

18. Mandic M, Castelli F, Janjic B, et al. One NY-ESO-1-derived epitope that promiscuously binds to multiple HLA-DR and HLA-DP4 molecules and stimulates autologous CD4+ T cells from patients with NY-ESO-1-expressing melanoma. *J Immunol*. 2005;174:1751-1759.

19. Sidney J, Steen A, Moore C, et al. Five HLA-DP molecules frequently expressed in the worldwide human population share a common HLA supertypic binding specificity. *J Immunol*. 2010;184:2492-2503.

20. Zeng G, Wang X, Robbins PF, Rosenberg SA, Wang RF. CD4(+) T cell recognition of MHC class II-restricted epitopes from NY-ESO-1 presented by a prevalent HLA DP4 allele: association with NY-ESO-1 antibody production. *Proc Natl Acad Sci U S A*. 2001;98:3964-3969.

21. Li F, Zhu MM, Niu BW, et al. Generation and expression analysis of BAC humanized mice carrying HLA-DP401 haplotype. *Animal Model Exp Med*. 2021;4:116-128.

22. Lakso M, Pichel JG, Gorman JR, et al. Efficient in vivo manipulation of mouse genomic sequences at the zygote stage. *Proc Natl Acad Sci U S A*. 1996;93:5860-5865.

23. Hashimoto K, Joshi SK, Koni PA. A conditional null allele of the major histocompatibility IA-beta chain gene. *Genesis*. 2002;32:152-153.

24. Bubeck Wardenburg J, Patel RJ, Schneewind O. Surface proteins and exotoxins are required for the pathogenesis of *Staphylococcus aureus* pneumonia. *Infect Immun*. 2007;75:1040-1044.

25. Livak KJ, Schmittgen TD. Analysis of relative gene expression data using real-time quantitative PCR and the 2(-Delta Delta C(T)) method. *Methods*. 2001;25:402-408.

26. Zhu MM, Niu BW, Liu LL, et al. Development of a humanized HLA-A30 transgenic mouse model. *Animal Model Exp Med*. 2022;5(4):350-361.

27. Cimolai N, Taylor GP, Mah D, Morrison BJ. Definition and application of a histopathological scoring scheme for an animal model of acute *Mycoplasma pneumoniae* pulmonary infection. *Microbiol Immunol*. 1992;36:465-478.

28. Lee AC, Zhang AJ, Chan JF, et al. Oral SARS-CoV-2 inoculation establishes subclinical respiratory infection with virus shedding in golden Syrian hamsters. *Cell Rep Med*. 2020;1:100121.

29. Wawegama NK, Markham PF, Elso CM, et al. Autoimmune-disease-prone NOD mice help to reveal a new genetic locus for reducing pulmonary disease caused by *Mycoplasma pulmonis*. *Infect Immun*. 2018;86:e00812-17.

30. Tuffs SW, Haeryfar SMM, McCormick JK. Manipulation of innate and adaptive immunity by staphylococcal superantigens. *Pathogens*. 2018;7:53.

31. Cheng S, Smart M, Hanson J, David CS. Characterization of HLA DR2 and DQ8 transgenic mouse with a new engineered mouse class II deletion, which lacks all endogenous class II genes. *J Autoimmun*. 2003;21:195-199.

32. Horn J, Stelzner K, Rudel T, Fraunholz M. Inside job: *Staphylococcus aureus* host-pathogen interactions. *Int J Med Microbiol*. 2018;308:607-624.

33. Pidwill GR, Gibson JF, Cole J, Renshaw SA, Foster SJ. The role of macrophages in *Staphylococcus aureus* infection. *Front Immunol*. 2020;11:620339.

34. Evren E, Ringqvist E, Willinger T. Origin and ontogeny of lung macrophages: from mice to humans. *Immunology*. 2020;160:126-138.

35. Dohlsten M, Bjorklund M, Sundstedt A, Hedlund G, Samson D, Kalland T. Immunopharmacology of the superantigen staphylococcal enterotoxin A in T-cell receptor V beta 3 transgenic mice. *Immunology*. 1993;79:520-527.

36. Dietert K, Gutbier B, Wienhold SM, et al. Spectrum of pathogen- and model-specific histopathologies in mouse models of acute pneumonia. *PLoS One*. 2017;12:e0188251.

37. Ting JP, Trowsdale J. Genetic control of MHC class II expression. *Cell*. 2002;109 Suppl:S21-S33.

38. Andersson G. Evolution of the human HLA-DR region. *Front Biosci*. 1998;3:d739-d745.

39. Rajagopalan G, Polich G, Sen MM, et al. Evaluating the role of HLA-DQ polymorphisms on immune response to bacterial superantigens using transgenic mice. *Tissue Antigens*. 2008;71:135-145.

40. McLoughlin RM, Lee JC, Kasper DL, Tzianabos AO. IFN-gamma regulated chemokine production determines the outcome of *Staphylococcus aureus* infection. *J Immunol*. 2008;181:1323-1332.

41. Miretti MM, Walsh EC, Ke X, et al. A high-resolution linkage-disequilibrium map of the human major histocompatibility complex and first generation of tag single-nucleotide polymorphisms. *Am J Hum Genet*. 2005;76:634-646.

42. Chen Z, de Kauwe AL, Keech C, et al. Humanized transgenic mice expressing HLA DR4-DQ3 haplotype: reconstitution of phenotype and HLA-restricted T-cell responses. *Tissue Antigens*. 2006;68:210-219.

43. Kimura K, Miyazaki S, Tateda K, Matsumoto T, Tsujimoto S, Yamaguchi K. Factors affecting the course and severity of transnasally induced *Staphylococcus aureus* pneumonia in mice. *J Med Microbiol*. 1999;48:1005-1010.

44. Bhakdi S, Tranum-Jensen J. Alpha-toxin of *Staphylococcus aureus*. *Microbiol Rev*. 1991;55:733-751.

45. Mazmanian SK, Ton-That H, Su K, Schneewind O. An iron-regulated sortase anchors a class of surface protein during *Staphylococcus aureus* pathogenesis. *Proc Natl Acad Sci U S A*. 2002;99:2293-2298.

46. McElroy MC, Harty HR, Hosford GE, Boylan GM, Pittet JF, Foster TJ. Alpha-toxin damages the air-blood barrier of the lung in a rat model of *Staphylococcus aureus*-induced pneumonia. *Infect Immun*. 1999;67:5541-5544.

47. Parker D, Ryan CL, Alonzo F 3rd, Torres VJ, Planet PJ, Prince AS. CD4+ T cells promote the pathogenesis of *Staphylococcus aureus* pneumonia. *J Infect Dis*. 2015;211:835-845.

SUPPORTING INFORMATION

Additional supporting information can be found online in the Supporting Information section at the end of this article.